
Can Population III stars be major origins of both merging binary black holes and extremely metal poor stars?

Ataru TANIKAWA¹, Gen CHIAKI², Tomoya KINUGAWA³, Yudai SUWA^{1,4,5} and Nozomu TOMINAGA^{6,7,8}

¹Department of Earth Science and Astronomy, Graduate School of Arts and Sciences, The University of Tokyo, 3-8-1 Komaba, Meguro-ku, Tokyo 153-8902, Japan

²Astronomical Institute, Graduate School of Science, Tohoku University, Aoba, Sendai 980-8578, Japan

³Institute for Cosmic Ray Research, The University of Tokyo, Kashiwa, Chiba 277-8582, Japan

⁴Department of Astrophysics and Atmospheric Sciences, Faculty of Science, Kyoto Sangyo University, Kyoto 603-8555, Japan

⁵Center for Gravitational Physics, Yukawa Institute for Theoretical Physics, Kyoto University, Kyoto 606-8502, Japan

⁶National Astronomical Observatory of Japan, National Institutes of Natural Sciences, 2-21-1 Osawa, Mitaka, Tokyo 181-8588, Japan

⁷Department of Physics, Faculty of Science and Engineering, Konan University, 8-9-1 Okamoto, Kobe, Hyogo 658-8501, Japan

⁸Kavli Institute for the Physics and Mathematics of the Universe (WPI), The University of Tokyo, 5-1-5 Kashiwanoha, Kashiwa, Chiba 277-8583, Japan

*E-mail: tanikawa@ea.c.u-tokyo.ac.jp

Received ; Accepted

Abstract

Population (Pop) III stars, first stars, or metal-free stars are made of primordial gas. We have examined if they can be dominant origins of merging binary black holes (BHs) and extremely metal-poor stars. The abundance pattern of EMP stars is helpful to trace back the properties of Pop III stars. We have confirmed previous arguments that the observed BH merger rate needs Pop III star formation efficiency 10 times larger than theoretically predicted values, while the cosmic reionization history still permits such a high Pop III star formation efficiency. On the other hand, we have newly found that the elemental abundance pattern of EMP stars only allows the Pop III initial mass function with the minimum mass of $\sim 15 - 27 M_{\odot}$. In other words, the minimum mass must not deviate largely from the critical mass below and above which Pop III stars leave behind neutron stars and BHs, respectively. Pop III stars may be still a dominant origin of merging binary BHs but our study has reduced the allowed parameter space under a hypothesis that EMP stars are formed from primordial gas mixed with Pop III supernova ejecta.

Key words: stars: Population II — stars: Population III — stars: black holes — gravitational waves

1 Introduction

Recently, a large number of black hole (BH) mergers have been detected by gravitational wave (GW) observations (Abbott et al. 2019; Abbott et al. 2021; The LIGO Scientific Collaboration et al. 2021a). Many formation scenarios of such BH mergers have been suggested: isolated binary evolution of Population I/II (Pop I/II) stars (Bethe & Brown 1998; Belczynski et al. 2007; Belczynski et al. 2016a; Mapelli et al. 2017; Eldridge et al. 2017; Ablimit & Maeda 2018; Eldridge et al. 2019; Mapelli et al. 2019; Belczynski et al. 2020; Olejak et al. 2020; Santoliquido et al. 2021; García et al. 2021), dynamical interactions in globular clusters (Kulkarni et al. 1993; Sigurdsson & Hernquist 1993; Portegies Zwart & McMillan 2000; Banerjee et al. 2010; Downing et al. 2010; Tanikawa 2013; Fujii et al. 2017; Askar et al. 2017; Park et al. 2017; Rodriguez et al. 2018; Samsing et al. 2018; Hong et al. 2020; Kimball et al. 2021; Wang et al. 2021; Anagnostou et al. 2020; Arca-Sedda et al. 2021), star clusters (Ziosi et al. 2014; Banerjee 2017; Fishbach et al. 2017; Gerosa & Berti 2017; Rastello et al. 2019; Kumamoto et al. 2020; Di Carlo et al. 2020; Kremer et al. 2020; Trani et al. 2021b; Fragione & Banerjee 2021), and galactic centers (O’Leary et al. 2009; Antonini & Perets 2012; VanLandingham et al. 2016; Bartos et al. 2017; Petrovich & Antonini 2017; Stone et al. 2017; Hoang et al. 2018; Hamers et al. 2018; McKernan et al. 2018; Leigh et al. 2018; Yang et al. 2019; Rasskazov & Kocsis 2019; Tagawa et al. 2020; McKernan et al. 2020; Arca Sedda 2020; Mapelli et al. 2021; Gerosa & Fishbach 2021; Liu & Bromm 2021), secular evolution in multiple stellar systems (Antonini et al. 2014; Silsbee & Tremaine 2017; Rodriguez & Antonini 2018; Liu & Lai 2019; Fragione & Kocsis 2019; Hamers & Safarzadeh 2020; Fragione et al. 2020; Britt et al. 2021; Trani et al. 2021a), hybrid channels of binary evolution and dynamical interactions (Bouffanais et al. 2021), and primordial BHs (Franciolini et al. 2021).

The first-generation metal-free (Population or Pop III) stars are typically massive (10–1000 M_{\odot}) (Omukai & Nishi 1998; Abel et al. 2002; Bromm & Larson 2004; Yoshida et al. 2008; Hosokawa et al. 2011; Stacy et al. 2011; Susa 2013; Hirano et al. 2014), and thus leave behind BHs more efficiently than Pop I/II stars. Thus, Pop III stars can contribute to the formation of merging BHs (Kinugawa et al. 2014; Hartwig et al. 2016; Belczynski et al. 2017; Tanikawa et al. 2021b; Liu & Bromm 2020a). Moreover, several rare GW events can be explained by Pop III stars. For example, a GW event with a 2.6 M_{\odot} compact object GW190814 (Abbott et al. 2020b) can be explained by Pop III remnant mergers (Kinugawa et al. 2021b). GW190521 with a BH in the pair instability (PI) mass gap (Abbott et al. 2020a; Abbott et al. 2020c; but see Fishbach & Holz 2020) can be formed from Pop III stars (Liu & Bromm 2020b; Kinugawa et al. 2021a; Farrell et al. 2021; Tanikawa et al. 2021a; Tanikawa et al. 2021c). Next-generation GW ob-

servatories, such as Cosmic Explorer (Reitze et al. 2019) and Einstein telescope (Punturo et al. 2010), may detect Pop III BHs more massive than 100 M_{\odot} (Belczynski et al. 2004; Hijikawa et al. 2021).

However, there is a debate whether Pop III stars are a major origin of observed BH mergers. Kinugawa et al. (2021c) have claimed that Pop III stars are a major origin of observed BH mergers with more than 20 M_{\odot} (hereafter, Pop III BH merger scenario). On the other hand, Hartwig et al. (2016) (see also Tanikawa et al. 2021b; Liu et al. 2021a) have argued that the merger rate of Pop III BHs should be much lower than observed. This debate comes from adopted Pop III formation rate. The former study has supposed the total Pop III mass in the local universe to be $\sim 10^{15} M_{\odot} \text{ Gpc}^{-3}$, which is the upper limit constrained by the cosmic reionization (de Souza et al. 2011; Inayoshi et al. 2016; Inayoshi et al. 2021). The latter studies have chosen it as $\sim 10^{13} M_{\odot} \text{ Gpc}^{-3}$ obtained by theoretical studies of Pop III star formation (Magg et al. 2016; Skinner & Wise 2020; Visbal et al. 2020). It is difficult to determine Pop III formation rate, since no Pop III star has been discovered so far (Frebel & Norris 2015; Magg et al. 2019).

In this paper, we suggest extremely metal-poor (EMP) stars as another approach to examine if Pop III stars may be a major origin of observed BH mergers. EMP stars are thought as stars with $[\text{Fe}/\text{H}] \lesssim -3$ and considered to form in gas clouds enriched by one or several supernovae (SNe) of Pop III stars (Audouze & Silk 1995; Ryan et al. 1996; Cayrel et al. 2004; Frebel & Norris 2015).¹ The metal contents and elemental abundances of EMP stars are crucial to trace back the properties of Pop III stars. EMP stars can be divided into two types: carbon-normal EMP stars and carbon-rich EMP stars (or carbon-enhanced metal-poor stars, CEMP stars) (Beers & Christlieb 2005). Carbon-normal EMP stars have elemental abundance patterns similar to the Sun. On the other hand, carbon-rich EMP stars have higher carbon abundances than the Sun ($[\text{C}/\text{Fe}] > 0.7$) (Aoki et al. 2007). The abundance ratio of carbon-rich stars to carbon-normal stars increases with $[\text{Fe}/\text{H}]$ decreasing (Beers & Christlieb 2005; Yong et al. 2013).

The presence of the two types can be interpreted as follows. Elemental abundances of carbon-normal EMP stars can best fit with the models of *successful* core-collapse supernovae (CCSNe). To explain the origin of carbon-rich stars, Umeda & Nomoto (2003) have proposed a so-called faint SN model: inner layers of stellar core falls back into central compact remnants, and only outer layers containing light elements, such as carbon, are ejected. However, in their model, mass cut is a free parameter to reproduce the elemental abundance of carbon-rich stars. Fryer et al. (2012) have independently found that a considerable fraction of ejecta falls back into a proto-neutron stars

¹ $[X/Y] = \log(n_X/n_Y) - \log(n_X/n_Y)_{\odot}$, where n_X and is the number density of an element X.

in a window of progenitor mass 20–30 M_{\odot} . Such *failed* supernovae (FSNe) leave behind a BH and should eject only carbon-rich outer layers. There is a firm evidence that a CEMP star is formed from the mixture of primordial gas and the ejecta of FSNe (Ito et al. 2013). These studies motivate us to define CCSNe and FSNe as the progenitors of carbon-normal and carbon-rich EMP stars, respectively. If primordial gas in dark matter minihalos (hereafter, minihalos) is enriched by carbon-normal and carbon-rich materials, the minihalos form carbon-normal and carbon-rich EMP stars, respectively. Note that there are many other scenarios of carbon-rich star formations: abundant production of carbon in supermassive rapidly rotating stars (Fryer et al. 2001; Liu et al. 2021b), enrichment of a Pop III star from asymptotic giant branch winds (Suda et al. 2004; Campbell et al. 2010), and interstellar medium accretion of gas decoupled from dust (Johnson 2015).

The purpose of this paper is to assess the Pop III BH merger scenario, under a hypothesis that EMP stars consist of primordial gas and Pop III supernova ejecta. Here, we remark the importance of this purpose. Although many formation scenarios of BH mergers have been proposed as described above, they have not yet been critically verified, and none of them has been rejected. Moreover, several studies have suggested that binary BHs can have multiple origins (Bouffanais et al. 2021; Zevin et al. 2021; Ng et al. 2021; Hütsi et al. 2021). As the first step, we need to narrow down promising formation scenarios of BH mergers, and scrutinize these formation scenarios one by one. In particular, we focus on Pop III stars, since they can be the origin of binary BHs with $\sim 30 M_{\odot}$ (Kinugawa et al. 2014; Kinugawa et al. 2021c), or with PI mass gap BHs (Tanikawa et al. 2021a). Among the scenarios of Pop III star origins, we pay attention to the Pop III BH merger scenario suggested by Kinugawa et al. 2014 and Kinugawa et al. 2021c. Since this scenario assumes the largest Pop III star mass in total among all the BH scenarios requiring Pop III stars, it would be easiest to get constrained. We also attribute CCSNe and FSNe to the formation of EMP stars, although there are several scenarios to explain the formation of EMP stars. This is because this EMP formation scenario can explain the abundance pattern of EMP stars (Ito et al. 2013) as described above.

The structure of this paper is as follows. In section 2, we present our method to obtain the merger rate of Pop III BHs, and the abundance ratio of carbon-rich EMP stars to carbon-normal EMP stars. In sections 3 and 4, we show our results, and summarize this paper, respectively.

2 Method

In this section, we present a method to obtain the merger rate of Pop III BHs, and the abundance ratio of carbon-rich EMP stars to carbon-normal EMP stars. In section 2.1, we describe

our Pop III star formation model. In section 2.2, we review our binary population synthesis model to derive the merger rate of Pop III BHs. In section 2.3, we show our EMP star formation model based on the results of binary population synthesis calculations. In section 2.4, we describe the necessary conditions satisfying GW and EMP observations.

2.1 Pop III star formation model

We assume that Pop III stars are born in minihalos. The minihalos are supposed to have $\sim 10^6 M_{\odot}$ and be formed at the high-redshift universe, $z \gtrsim 5$ (Hartwig et al. 2016; Skinner & Wise 2020; Visbal et al. 2020). We adopt the number density of the minihalos in the local universe (n_{halo}), such that $n_{\text{halo}} \sim 10^{11} \text{ Gpc}^{-3}$. We obtain this number density from the results of Skinner & Wise (2020); their figure 4 shows that the total mass of Pop III stars formed in each 1 cubic Gpc is $\sim 3 \times 10^{13} M_{\odot} \text{ Gpc}^{-3}$, and their figure 8 indicates that the total mass of Pop III stars in each minihalo (\bar{M}) is $\sim 300 M_{\odot}$ on average. We basically refer to the Pop III formation model of Skinner & Wise (2020). Although we adopt the model of Skinner & Wise (2020), we note that many research groups have studied the Pop III formation in the universe (Susa et al. 2014; Hirano et al. 2015; Ishiyama et al. 2016; Inayoshi et al. 2016; Magg et al. 2016; Visbal et al. 2020).

We construct the mass function of the total mass of Pop III stars in each minihalo (M), expressed as

$$f_1(M) \propto M^{-1} (0.1M_{\text{max}} < M < M_{\text{max}}). \quad (1)$$

We get this mass function, simplifying that of Skinner & Wise (2020) (see their figure 8) for ease of handling. Their mass function can be interpreted as logarithmic flat over a single digit (from $\sim 50M_{\odot}$ to $\sim 500M_{\odot}$). We ignore that a small fraction of minihalos form $\lesssim 50M_{\odot}$ Pop III stars in total. We treat the maximum mass of Pop III stars in total (M_{max}) as a free parameter, although $M_{\text{max}} \sim 500M_{\odot}$ in Skinner & Wise (2020). A reason for this treatment is that Pop III star formation models in each minihalo still have uncertainties in baryon physics, such as magnetic field, turbulence, and so on (Federrath et al. 2011; Turk et al. 2012; Sadanari et al. 2021; Higashi et al. 2021). Moreover, we practically need Pop III stars enough to explain the observed BH merger rate.

We suppose that all the Pop III stars are born at the same time at the high-redshift of $\gtrsim 5$. We set the binary fraction of Pop III stars to 1. This is because Pop III stars are usually born in multiple stellar systems (Turk et al. 2009; Clark et al. 2011b; Greif et al. 2011; Susa et al. 2014; Sugimura et al. 2020).

The initial mass function (IMF) of primary stars is expressed as

$$f_2(m_1) \propto m_1^{-1} (m_{\text{min}} < m_1 < 150M_{\odot}). \quad (2)$$

The distribution is logarithmically flat, which is consistent with

Susa et al. (2014) and Hirano et al. (2014). Although a part of Pop III stars may have more than $150 M_{\odot}$ (but see Tarumi et al. 2020), we do not take into account them conservatively. Note that such Pop III stars form more massive than $100 M_{\odot}$ BHs, and thus do not contribute to the observed BH merger rate. We regard the minimum mass of Pop III stars as a free parameter. This parameter has large effects on the elemental abundance pattern of EMP stars.

Binary parameters we adopt are the same as those proposed by Sana et al. (2012). The mass ratio of companion stars to primary stars (q) can be expressed as

$$f_3(q) \propto q^{-0.1} (0.1 < q < 1). \quad (3)$$

Note that the minimum mass of the companion stars is also m_{\min} . The binary period (P) and eccentricity (e) distribution are, respectively, given by

$$f_4(\log P) \propto (\log P)^{-0.55} (0.15 < \log(P/\text{day}) < 5.5), \quad (4)$$

and

$$f_5(e) \propto e^{-0.42} (0 < e < 1). \quad (5)$$

Note that the minimum and maximum periods are the same as those of de Mink & Belczynski 2015.

2.2 Merging BH formation model

We generate 10^6 binary stars with the primary IMF and binary parameters described in section 2.1. We follow the evolution of the binary stars, using binary population synthesis technique. We calculate the BH merger rate density in the current universe (R) as

$$R = \frac{\rho_3}{\mathcal{M}_{\text{sim}}} \frac{\mathcal{N}_{\text{sim}}(t_d)}{\Delta t_d}, \quad (6)$$

where ρ_3 is the total mass of Pop III stars formed in each unit volume, \mathcal{M}_{sim} is the total mass of the simulated binary stars, t_d is the delay time of BH mergers from Pop III star formation, and $\mathcal{N}_{\text{sim}}(t_d)$ is the total number of BH mergers with the delay time from t_d to $t_d + \Delta t_d$ in the simulations. We set $t_d = 10$ Gyr and $\Delta t_d = 5$ Gyr, since Pop III stars are born in the early universe. As described later, we focus on BH mergers with the heavier mass of $20 - 40 M_{\odot}$. The BH merger rate can be calculated as

$$R_{20-40} = \frac{\rho_3}{\mathcal{M}_{\text{sim}}} \frac{\mathcal{N}_{\text{sim},20-40}(t_d)}{\Delta t_d}, \quad (7)$$

where $\mathcal{N}_{\text{sim},20-40}(t_d)$ is the total number of BH mergers with the heavier mass of $20 - 40 M_{\odot}$, and with the delay time from t_d to $t_d + \Delta t_d$ in the simulations.

Hereafter, we describe our binary population synthesis technique. We use a binary population synthesis code BSE with extensions to EMP stars (Tanikawa et al. 2020; Tanikawa et al. 2021b). Pop III stars evolve along with the fitting formulae of stars with stellar metallicity $Z = 10^{-8} Z_{\odot}$. The evolution of

$Z = 10^{-8} Z_{\odot}$ stars is the same as Pop III star evolution because of the low metallicity. We do not consider stellar wind mass loss because of zero metallicity. Our supernova model is based on the rapid model of Fryer et al. (2012) with modifications of PI. The PI model is given by

$$m_{\text{rem}} = \begin{cases} m_{\text{rapid}} & (m_c \leq m_{c,\text{PPI}}) \\ m_{c,\text{PPI}} & (m_{c,\text{PPI}} < m_c \leq m_{c,\text{PISN}}) \\ 0 & (m_{c,\text{PISN}} < m_c \leq m_{c,\text{DC}}) \\ m_{\text{rapid}} & (m_c > m_{c,\text{DC}}) \end{cases}, \quad (8)$$

where m_{rem} is the remnant mass, m_{rapid} is the remnant mass without the PI model, and m_c is the helium core mass. In the ascending order of the helium core mass, stars experience supernovae in the framework of the rapid model, pulsational PI (Heger & Woosley 2002; Woosley et al. 2007; Yoshida et al. 2016; Woosley 2017; Leung et al. 2019), PI supernovae (Barkat et al. 1967; Fraley 1968; Bond et al. 1984; El Eid & Langer 1986; Fryer et al. 2001; Heger & Woosley 2002; Umeda & Nomoto 2002; Kasen et al. 2011; Yoon et al. 2012), and collapse to a BH together with possible association with gamma-ray bursts (Fryer et al. 2001; Nakazato et al. 2006; Suwa et al. 2007a; Suwa et al. 2007b; Suwa et al. 2009; Suwa & Ioka 2011; Woosley & Heger 2012; Nakauchi et al. 2012; Uchida et al. 2019a; Uchida et al. 2019b). We adopt $(m_{c,\text{PPI}}, m_{c,\text{PISN}}, m_{c,\text{DC}}) = (45M_{\odot}, 65M_{\odot}, 135M_{\odot})$, which is similar to the model of Belczynski et al. (2016b). We do not account for BH natal kicks. BH natal kicks have small effects on merging binary BHs, since their binary motions are much faster than their natal kicks (Tanikawa et al. 2021b).

As described above, stars experience supernovae in the framework of the rapid model if $m_c \leq m_{c,\text{PPI}}$, or if $m_{z\text{ams}} \lesssim 80 M_{\odot}$, where $m_{z\text{ams}}$ is zero-age main sequence (ZAMS) mass. The supernovae can be divided into three types by $m_{z\text{ams}}$. For $m_{z\text{ams}} \lesssim 20 M_{\odot}$, stars leave behind neutron stars with supernova ejecta. We regard that these stars cause CCSNe. For $20 \lesssim m_{z\text{ams}} \lesssim 30 M_{\odot}$, stars leave behind BHs with supernova ejecta. We regard that these stars cause FSNe. For $30 \lesssim m_{z\text{ams}}/M_{\odot} \lesssim 80$, stars leave behind BHs without supernova ejecta, which can be interpreted as direct collapse.

Our binary evolution model is based on the BSE code (Hurley et al. 2002). We describe the difference between the original BSE and our models. In the original BSE model, core helium burning and shell helium burning stars are assumed to have radiative and convective envelopes, respectively. On the other hand, in our model, stars with $\log(T_{\text{eff}}/K) \geq 3.65$ and < 3.65 are assumed to have radiative and convective envelopes, respectively, where T_{eff} is the effective temperature of a star. The original BSE and our models have different formulae of tidal interaction for stars with radiative envelopes. The original BSE model adopts the formulae of Zahn (1975), while our model adopts the formulae of Kinugawa et al. (2021c), based on Yoon et al. (2010) and Qin et al. (2018). The mass transfer rate in Roche-

lobe overflow is calculated by the formulae of Kinugawa et al. (2021c), based on Paczyński & Sienkiewicz (1972), Savonije (1978), Edwards & Pringle (1987), and Inayoshi et al. (2017). The common-envelope evolution is modeled as α formalism (Webbink 1984). We adopt $\alpha_{\text{CE}} = 1$ and calculate λ_{CE} from Claeys et al. (2014). We omit magnetic braking, since the magnetic field of first stars is expected to be weaker than that of Pop I/II stars (Pudritz & Silk 1989; Doi & Susa 2011) and the dominant component of the magnetic field is tangled according to Sharda et al. (2020).

2.3 EMP star formation model

We suppose that EMP stars are born in minihalos (Chiaki et al. 2020) and made of primordial gas enriched by Pop III CCSNe and FSNe. We focus only on whether EMP stars are carbon-rich or carbon-normal. Thus, we take into account chemical elements of hydrogen, carbon, and iron.

Each minihalo has the following elemental abundance after all the Pop III stars in the minihalo finish their evolution. Each minihalo has $10^5 M_{\odot}$ hydrogen. When a Pop III star causes a CCSN, it ejects $0.2 M_{\odot}$ carbon and $0.07 M_{\odot}$ iron (Nomoto et al. 2013). When a Pop III star causes a FSN, it ejects $0.989 M_{\odot}$ carbon and $1.47 \times 10^{-5} M_{\odot}$ iron (Marassi et al. 2014). When a Pop III star experiences pulsational PI, it ejects no carbon or iron, since its carbon core is intact (Umeda et al. 2020). When a Pop III star experiences a PI supernova, it disrupts the minihalo because of its large explosion energy, and thus the minihalo cannot form EMP stars (Greif et al. 2007; Cooke & Madau 2014; Chiaki et al. 2018).

We regard that the number ratio of carbon-rich EMP stars to carbon-normal EMP stars is equal to that of carbon-rich minihalos to carbon-normal minihalos. In other words, we assume that chemical elements are completely mixed in each minihalo, and that all the minihalos form EMP stars with the same number and IMF. We adopt these conditions for simplicity, although IMF of EMP stars can depend on metallicity (Omukai 2000; Schneider et al. 2003; Dopcke et al. 2013; Chiaki et al. 2016; Chon et al. 2021).

2.4 Necessary conditions from Pop III, GW and EMP observations

In this section, we describe three necessary conditions where Pop III stars are major origins of merging BHs whose masses are 20–40 M_{\odot} , and EMP stars are formed from primordial gas mixed with Pop III supernova ejecta. The three necessary conditions are as follows.

1. $\rho_3 \leq 10^{15} M_{\odot} \text{ Gpc}^{-3}$
2. $3 \leq R_{20-40} / (\text{yr}^{-1} \text{ Gpc}^{-3}) \leq 30$
3. $0.01 \leq f_{\text{c-rich}} \leq 1$

We explain these conditions in detail later.

We set the first necessary condition to impose an upper limit on ρ_3 , the total mass of Pop III stars formed in each 1 cubic Gpc until now. The upper limit is $10^{15} M_{\odot} \text{ Gpc}^{-3}$. More than the upper limit cannot be permitted by reionization constraints (Inayoshi et al. 2016; Inayoshi et al. 2021).

We need the second necessary condition to regard Pop III BHs as a major origin of observed BH mergers. Kinugawa et al. (2021c) have argued that Pop III BHs can form all the observed BH mergers with the primary masses of $> 20 M_{\odot}$. We do not take into account BH mergers with more than 40 M_{\odot} for the second necessary condition. There are two reasons. First, we can say that the Pop III BH merger scenario should be successful, if the second necessary condition is satisfied. Second, a BH merger rate with more than 40 M_{\odot} strongly depends on uncertainties of the PI model (Farmer et al. 2020; Belczynski 2020; Costa et al. 2021). The second necessary condition may be strict more than necessary. As a reference, we investigate the case where this condition is relaxed to $R_{20-40} = 1 - 100 \text{ yr}^{-1} \text{ Gpc}^{-3}$.

We adopt the third necessary condition under which the number ratio of carbon-rich EMP stars to carbon-normal EMP stars, $f_{\text{c-rich}}$, is consistent with EMP observations. We define EMP stars as those with $[\text{Fe}/\text{H}] \leq -2.5$. Moreover, we define carbon-rich and carbon-normal EMP stars as those with $[\text{C}/\text{Fe}] > 2$ and < 2 , respectively, following Chiaki et al. (2017) (see also Yoon et al. 2016). According to the SAGA database (Suda et al. 2008), $f_{\text{c-rich}} \sim 0.05$. We do not impose a strict condition on $f_{\text{c-rich}}$. Rather, we allow $f_{\text{c-rich}}$ to have wide range of values, such that $f_{\text{c-rich}}$ ranges over 2 digits. This is because we obtain $f_{\text{c-rich}} \sim 0.05$ directly from the SAGA database, ignoring selection bias. If we take into account the completeness of EMP star observations, we may take the necessary condition more strictly. Eventually, we can narrow the allowed region. However, this is beyond of the scope of this paper.

3 Results

Figure 1 shows which $(m_{\text{min}}, M_{\text{max}})$ satisfies the three necessary conditions described in section 2.4. We first focus on M_{max} . We need $M_{\text{max}} \lesssim 3 \times 10^4 M_{\odot}$ in order to satisfy the first necessary condition. We also need $M_{\text{max}} \gtrsim 10^4 M_{\odot}$. Otherwise, the second necessary condition cannot be satisfied, since the Pop III BH merger rate density is too small: $R_{20-40} < 3 \text{ yr}^{-1} \text{ Gpc}^{-3}$. This M_{max} is much larger than $M_{\text{max}} \sim 600 M_{\odot}$ obtained by numerical simulations of Skinner & Wise (2020). Similar things have been already pointed out by Hartwig et al. (2016). Nevertheless, we have to note that the first necessary condition is not still violated even when the second necessary condition is satisfied.

We next focus on m_{min} . We need $15 \lesssim m_{\text{min}}/M_{\odot} \lesssim 27$

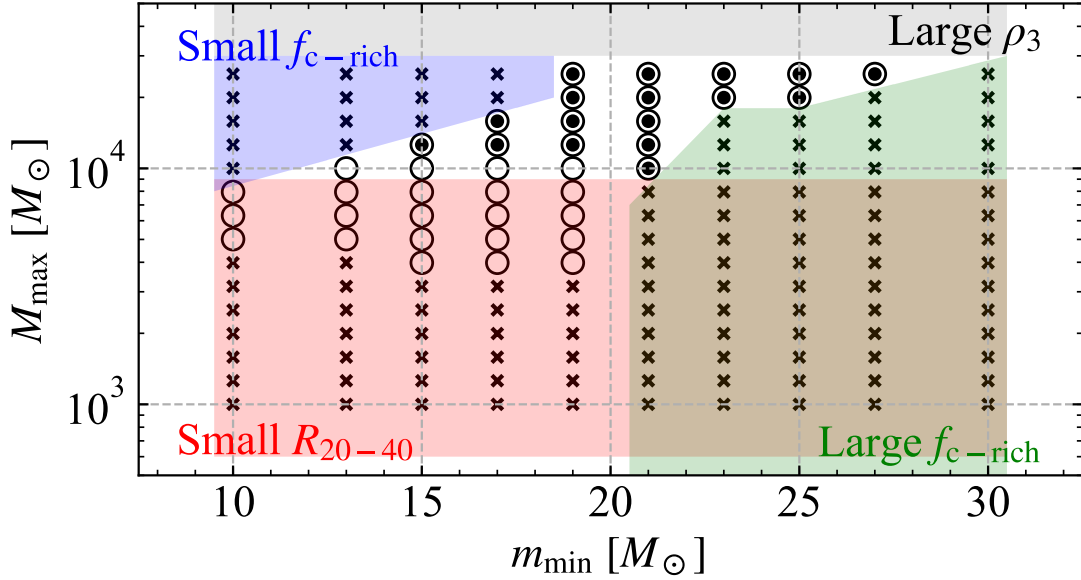


Fig. 1. Combinations of m_{\min} and M_{\max} which satisfy the three necessary conditions described in section 2.4. m_{\min} and M_{\max} are the minimum mass of the primary stellar IMF, the maximum mass for the mass function of the total mass of Pop III stars in each halo, respectively. The combinations indicated by open circles with dots satisfy all the necessary conditions. Those indicated by open circles do so, when the second necessary condition is relaxed to $1 < R_{20-40}/(\text{yr}^{-1}\text{Gpc}^{-3}) < 10^2$. Those indicated by crosses do not. Shaded regions indicate which necessary condition the combinations do not satisfy. In the red, blue, green, and gray regions, R_{20-40} is smaller, $f_{c\text{-rich}}$ is smaller, $f_{c\text{-rich}}$ is larger, and ρ_3 is larger than the corresponding necessary conditions, respectively.

Table 1. (m_{\min}, M_{\max}) chosen for Figures 2, 3, and 4, where m_{\min} and M_{\max} are the minimum mass of the primary stellar IMF and the maximum mass for the mass function of the total mass of Pop III stars in each halo, respectively.

Figure	m_{\min}	M_{\max}
Figure 2	$10 M_{\odot}$	$600 M_{\odot}$
Figure 3	$10 M_{\odot}$	$15000 M_{\odot}$
Figure 4	$17 M_{\odot}$	$12000 M_{\odot}$

in order to satisfy the third necessary condition. The allowed M_{\max} becomes narrower when m_{\min} deviates from $\sim 20M_{\odot}$, the boundary mass between CCSNe and FSNe. If m_{\min} is too small, $f_{c\text{-rich}} < 0.01$, since minihalos have a large number of CCSNe, get iron elements, and cannot form carbon-rich EMP stars. If m_{\min} is too large, $f_{c\text{-rich}} > 1$, since minihalos have a small number of CCSNe, get little iron element, and cannot form carbon-normal EMP stars.

If we relax the second necessary condition from $3 \leq R_{20-40}/(\text{yr}^{-1}\text{Gpc}^{-3}) \leq 30$ to $1 \leq R_{20-40}/(\text{yr}^{-1}\text{Gpc}^{-3}) \leq 100$, the allowed region becomes wider not only in the direction of M_{\max} , but also in the direction of m_{\min} . Especially, $m_{\min} = 10 M_{\odot}$ can be allowed. Each minihalo forms a smaller amount of Pop III stars in the latter case than in the former case. Each minihalo has CCSNe at a smaller probability, and gets a smaller amount of iron elements. Thus, some of minihalos can form carbon-rich EMP stars.

In order to complement the above explanations, we demonstrate how to satisfy the three necessary conditions. Table 1 shows our choice of (m_{\min}, M_{\max}) in advance. As the starting point, we choose $(m_{\min}, M_{\max}) = (10M_{\odot}, 600M_{\odot})$. The values of m_{\min} and M_{\max} are consistent with Susa et al. (2014) and Skinner & Wise (2020), respectively. Thus, these values are based on recent numerical simulations for Pop III star formations. The results are shown in Figure 2. In this case, the first and third conditions are satisfied. However, the BH merger rate is $R_{20-40} \sim 1.6 \times 10^{-1} \text{ yr}^{-1} \text{ Gpc}^{-3}$, which is much smaller than the second necessary condition. Thus, we need to change (m_{\min}, M_{\max}) to increase R_{20-40} .

In order to increase R_{20-40} , we set $(m_{\min}, M_{\max}) = (10M_{\odot}, 15000M_{\odot})$. Figure 3 shows the results for this case. The Pop III star formation rate is $\rho_3 \sim 5.9 \times 10^{14} M_{\odot} \text{ Gpc}^{-3}$. This is much larger than that of Skinner & Wise (2020), however does not still violate the first necessary condition. The large M_{\max} increases R_{20-40} to $\sim 3.1 \text{ yr}^{-1} \text{ Gpc}^{-3}$, consistent with the second necessary condition. On the other hand, $f_{c\text{-rich}} \ll 0.01$. This is much smaller than the third necessary condition. The reason why $f_{c\text{-rich}}$ decreases from the case of $(m_{\min}, M_{\max}) = (10M_{\odot}, 600M_{\odot})$ to $(10M_{\odot}, 15000M_{\odot})$ is as follows. In the case of $(m_{\min}, M_{\max}) = (10M_{\odot}, 15000M_{\odot})$, all the minihalos have a large number of Pop III stars with $m_{\text{zams}} \lesssim 20M_{\odot}$. They have many CCSNe, and are sufficiently polluted by iron. Thus, they form only carbon-normal EMP stars after that.

In order to increase $f_{c\text{-rich}}$, we adopt $(m_{\min}, M_{\max}) = (17M_{\odot}, 12000M_{\odot})$ as seen in Figure 4. In this case, the third necessary condition are satisfied as well as the first and second conditions. Since we increase m_{\min} , minihalos have Pop III stars with $m_{\text{zams}} \lesssim 20M_{\odot}$ and CCSNe at a small probability. Then, a significant fraction of minihalos are not polluted by iron. There are no EMP stars with $[\text{Fe}/\text{H}] \sim -6$ – -3 in our model in contrast to the observation of EMP stars. However, this may be reconciled when we take into account inhomogeneous mixing of Pop III supernova ejecta in minihalos.

In order to assess the Pop III BH merger scenario, previous studies have focused on the secondary necessary condition. Thus, they have only pointed out that minihalos should form a larger amount of Pop III stars than predicted theoretically by a factor of more than 10. In addition to that, we find a new constraint on m_{\min} : $15 \lesssim m_{\min}/M_{\odot} \lesssim 27$ by taking into account the third necessary condition. The allowed range M_{\max} becomes narrower when m_{\min} deviates from $\sim 20 M_{\odot}$. In other words, m_{\min} should be close to the critical mass where the fate of a Pop III star transits from a CCSN to a FSN. The critical mass is $\sim 20 M_{\odot}$ in our adopted supernova model. Otherwise, minihalos can form only one type of carbon-rich and carbon-normal EMP stars.

4 Summary and discussion

We examine the Pop III BH merger scenario under the hypothesis that EMP stars consist of primordial gas and Pop III supernova ejecta. We suppose that the scenario is valid if the following three necessary conditions are satisfied. First, Pop III formation rate is $\rho_3 \leq 10^{15} M_{\odot} \text{ Gpc}^{-3}$. Second, Pop III BHs merge at a rate of $3 \leq R_{20-40}/(\text{yr}^{-1} \text{ Gpc}^{-3}) \leq 30$. Third, EMP stars have the number ratio $0.01 \leq f_{c\text{-rich}} \leq 1$. In order to obtain Pop III BHs and EMP stars, we construct a simple formation model of Pop III stars, and simulate the evolution of Pop III stars by binary population synthesis technique.

We find that there is a region satisfying the three necessary conditions. The Pop III formation rate should be $\rho_3 \gtrsim 3 \times 10^{14} M_{\odot} \text{ Gpc}^{-3}$. This means that each minihalo should form Pop III stars with $M_{\max} \sim 10^4 M_{\odot}$, or $10^3 - 10^4 M_{\odot}$ in total. Although this formation rate does not violate the first necessary condition, it is much larger than numerically predicted by Skinner & Wise (2020). Similar things have been already pointed out by Hartwig et al. (2016).

We newly find that the minimum mass of Pop III stars should be $15 \lesssim m_{\min}/M_{\odot} \lesssim 27$. If $m_{\min}/M_{\odot} \lesssim 15$ or $m_{\min}/M_{\odot} \gtrsim 27$, $f_{c\text{-rich}}$ is smaller or larger than the third necessary condition, respectively. This is because each minihalo gets too much CCSNe and FSNe for $m_{\min}/M_{\odot} \lesssim 15$ and $m_{\min}/M_{\odot} \gtrsim 27$, respectively. Moreover, the allowed region becomes narrower with m_{\min} deviating from $\sim 20 M_{\odot}$, which is the boundary

mass between CCSNe and FSNe.

We compare the new constraint with m_{\min} obtained from numerical simulations. Susa et al. (2014) have shown that the number of Pop III stars is sharply decreased just below $\sim 10 M_{\odot}$. On the other hand, in Hirano et al. (2014) (see also Hirano et al. 2015), the number of $10 M_{\odot}$ Pop III stars is much smaller than that of $20 M_{\odot}$, which can be interpreted as $10 \lesssim m_{\min}/M_{\odot} \lesssim 20$. From these numerical simulations, we can regard $10 \lesssim m_{\min}/M_{\odot} \lesssim 20$, however cannot strictly determine m_{\min} . Thus, we do not exclude possibility of the Pop III BH merger scenario, under our assumption that EMP stars are formed from primordial gas mixed with Pop III supernova ejecta.

We have to note that recent studies have also found the formation of low-mass Pop III stars (Machida et al. 2008; Clark et al. 2011a; Clark et al. 2011b; Greif et al. 2011; Greif et al. 2012; Machida & Doi 2013; Susa et al. 2014; Chiaki et al. 2016). Such low-mass Pop III stars can have $\lesssim 1 M_{\odot}$. However, the number of such low-mass Pop III stars is much smaller than Pop III stars with $\gtrsim 10 M_{\odot}$. The presence of such low-mass Pop III stars can be negligible for our results.

We emphasize that the new constraint on m_{\min} ($15 \lesssim m_{\min}/M_{\odot} \lesssim 27$) is necessary only when we claim the Pop III BH merger scenario. Note that Pop III stars are a major origin of observed BH mergers with more than $20 M_{\odot}$ in the Pop III BH merger scenario. In other words, Pop III stars can have $\lesssim 15 M_{\odot}$ stars (say $10 M_{\odot}$ stars or less massive stars) if we do not adopt the Pop III merger scenario. The new constraint on m_{\min} can be applicable when we reconcile the Pop III BH merger scenario with $0.01 \leq f_{c\text{-rich}} \leq 1$.

Hereafter, we make caveats on our model. We treat M_{\max} as a free parameter, while we fix n_{halo} as $\sim 10^{11} \text{ Gpc}^{-3}$. However, M_{\max} and n_{halo} may be anti-correlated. Skinner & Wise (2020) have performed numerical simulations to follow cosmic chemical evolution as well as Pop III star formation. Since we assume that more Pop III stars are formed than Skinner & Wise (2020) expected, Pop III's surrounding gas should be polluted more rapidly. The pollution should stop forming Pop III stars earlier, and start forming Pop I/II stars earlier. Thus, if we assume that each minihalo yields a larger amount of Pop III stars than their results (i.e. $M_{\max} \gg 600 M_{\odot}$), we should decrease the number density of minihalos (i.e. $n_{\text{halo}} \ll 10^{11} \text{ Gpc}^{-3}$). In that case, the Pop III BH merger scenario should be difficult to be valid. In this paper, we do not take into account this, because we simply control Pop III star formation rate.

We prepare the three necessary conditions as described in section 2.4. It might be possible to add other necessary conditions. As for merging BHs, GW observations obtain not only BH masses but also BH spins. We might account for BH spins for necessary conditions. However, we do not do so. This is because the estimates of BH spins are less reliable and less con-

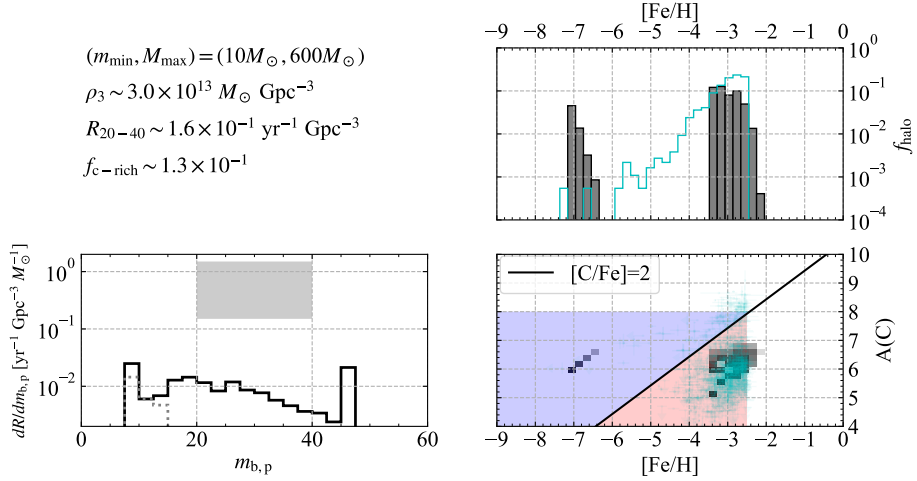


Fig. 2. (Top left) Input parameters of $(m_{\min}, M_{\max}) = (10M_{\odot}, 600M_{\odot})$, and resulting values of ρ_3 , R_{20-40} , and $f_{c\text{-rich}}$. (Bottom left) BH merger rate density differentiated by the heavier BH mass ($m_{b,p}$) in the local universe. Gray-shaded regions in the left panels show $3 < R_{20-40}/(\text{yr}^{-1} \text{Gpc}^{-3}) < 30$ if the $dR/dm_{b,p}$ distribution is assumed to be flat in this range. The dotted gray histograms indicate BH mergers either of which are formed through FSNe. FSNe form only light BHs. There are two local peaks at $m_1 \sim 10$ and $45 M_{\odot}$. The lower-mass peak is formed through the rapid model (Fryer et al. 2012) in which relatively low-mass progenitors ($20\text{--}30 M_{\odot}$ ZAMS stars) preferentially leave behind $5\text{--}10 M_{\odot}$ BHs. The higher-mass peak is formed by pulsational PI (see Eq. (8)). (Top right) $[\text{Fe}/\text{H}]$ distribution of minihalos after Pop III star evolution. The abundance of EMP stars is indicated by the cyan histograms normalized to unity. These data are retrieved from the SAGA database (Suda et al. 2008; Suda et al. 2011; Yamada et al. 2013; Suda et al. 2017). Our model do not obtain $-6 \lesssim [\text{Fe}/\text{H}] \lesssim -4$, since we do not take into account variation of FSNe unlike Tominaga et al. 2014. (Bottom right) Carbon ($A(C)$) and $[\text{Fe}/\text{H}]$ distribution of minihalos after Pop III star evolution. Blue and red-shaded regions in the right panels indicate the abundance of carbon-rich and carbon-normal EMP stars, respectively. The cyan points with error bars indicate EMP stars.

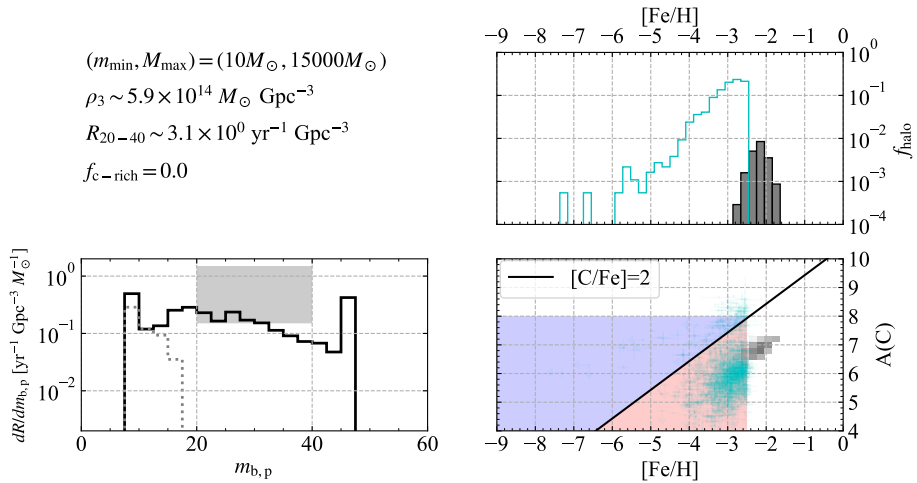


Fig. 3. The same as Figure 2 except for input parameters of $(m_{\min}, M_{\max}) = (10M_{\odot}, 15000M_{\odot})$. Two local peaks at $m_1 \sim 10$ and $45 M_{\odot}$ in the bottom left panel are formed through the same mechanisms as in Figure 2.

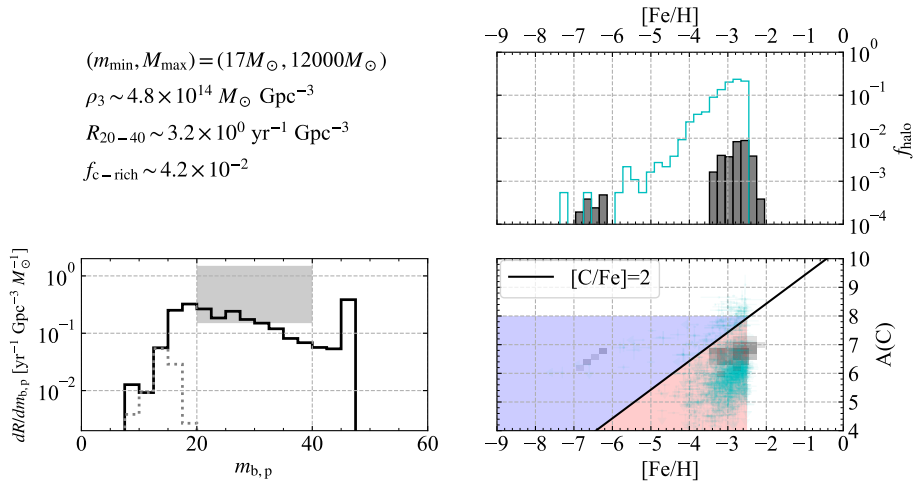


Fig. 4. The same as Figure 2 except for input parameters of $(m_{\min}, M_{\max}) = (17M_{\odot}, 12000M_{\odot})$. In the bottom left panel, the lower-mass peak is formed through the same mechanism as in Figure 2. The higher-mass peak in Figure 2 disappears in this figure, since the higher-mass peak needs many binary stars with $\lesssim 17 M_{\odot}$ secondary stars.

strained than BH masses (The LIGO Scientific Collaboration et al. 2021b). Thus, we adopt only BH masses for the necessary conditions. As for EMP stars, chemical elements other than carbon are also observed. Nevertheless, we do not take into account them. This is because carbon abundance is the most characteristic and most observed elements in EMP stars, and is the most sensitive to whether CCSNe or FSNe happen.

In our supernova model, Pop III stars with $m_{\text{zams}}/M_{\odot} \lesssim 20$ and $\gtrsim 20$ deterministically cause CCSNe and FSNe, respectively, except that binary interactions slightly change their fates. On the other hand, recent supernova studies have suggested that stars with $m_{\text{zams}} = 10 - 30 M_{\odot}$ cause CCSNe stochastically (Ugliano et al. 2012; Pejcha & Thompson 2015; Sukhbold et al. 2016; Müller et al. 2016; Sukhbold et al. 2018; Kresse et al. 2021). This may largely affect our results. However, we do not adopt such supernova models. This is because these models have not been prepared to use in binary population synthesis technique. These models tell us whether stars experience CCSNe or direct collapses to BHs, but do not include FSNe which is needed in binary population synthesis technique.

Acknowledgments

We thank organizers of the first star and first galaxy conference 2020 in Japan for giving us a good opportunity to start our collaboration. This study was supported in part by Grants-in-Aid for Scientific Research (19K03907, 20H00174, 20H01904, 21K13915) from the Japan Society for the Promotion of Science and Grants-in-Aid for Scientific Research on Innovative areas (17H06360, 18H05437, 20H04747) from the Ministry of Education, Culture, Sports, Science and Technology (MEXT), Japan.

References

Abbott, B. P., Abbott, R., Abbott, T. D., et al. 2019, *Physical Review X*,

- 9, 031040
 Abbott, R., Abbott, T. D., Abraham, S., et al. 2020a, *Phys. Rev. Lett.*, 125, 101102
 —. 2020b, *ApJL*, 896, L44
 —. 2020c, *ApJL*, 900, L13
 —. 2021, *Physical Review X*, 11, 021053
 Abel, T., Bryan, G. L., & Norman, M. L. 2002, *Science*, 295, 93
 Ablimit, I., & Maeda, K. 2018, *ApJ*, 866, 151
 Anagnostou, O., Trenti, M., & Melatos, A. 2020, *PASA*, 37, e044
 Antonini, F., Murray, N., & Mikkola, S. 2014, *ApJ*, 781, 45
 Antonini, F., & Perets, H. B. 2012, *ApJ*, 757, 27
 Aoki, W., Beers, T. C., Christlieb, N., et al. 2007, *ApJ*, 655, 492
 Arca Sedda, M. 2020, *ApJ*, 891, 47
 Arca-Sedda, M., Rizzuto, F. P., Naab, T., et al. 2021, *ApJ*, 920, 128
 Askar, A., Szkudlarek, M., Gondek-Rosińska, D., Giersz, M., & Bulik, T. 2017, *MNRAS*, 464, L36
 Audouze, J., & Silk, J. 1995, *ApJL*, 451, L49
 Banerjee, S. 2017, *MNRAS*, 467, 524
 Banerjee, S., Baumgardt, H., & Kroupa, P. 2010, *MNRAS*, 402, 371
 Barkat, Z., Rakavy, G., & Sack, N. 1967, *Phys. Rev. Lett.*, 18, 379
 Bartos, I., Kocsis, B., Haiman, Z., & Márka, S. 2017, *ApJ*, 835, 165
 Beers, T. C., & Christlieb, N. 2005, *ARA&A*, 43, 531
 Belczynski, K. 2020, *ApJL*, 905, L15
 Belczynski, K., Bulik, T., & Rudak, B. 2004, *ApJL*, 608, L45
 Belczynski, K., Holz, D. E., Bulik, T., & O’Shaughnessy, R. 2016a, *Nature*, 534, 512
 Belczynski, K., Ryu, T., Perma, R., et al. 2017, *MNRAS*, 471, 4702
 Belczynski, K., Taam, R. E., Kalogera, V., Rasio, F. A., & Bulik, T. 2007, *ApJ*, 662, 504
 Belczynski, K., Heger, A., Gladysz, W., et al. 2016b, *A&A*, 594, A97
 Belczynski, K., Klencki, J., Fields, C. E., et al. 2020, *A&A*, 636, A104
 Bethe, H. A., & Brown, G. E. 1998, *ApJ*, 506, 780
 Bond, J. R., Arnett, W. D., & Carr, B. J. 1984, *ApJ*, 280, 825
 Bouffanais, Y., Mapelli, M., Santoliquido, F., et al. 2021, *MNRAS*, 507, 5224
 Britt, D., Johanson, B., Wood, L., Miller, M. C., & Michaely, E. 2021, *MNRAS*, 505, 3844

- Bromm, V., & Larson, R. B. 2004, *ARA&A*, 42, 79
- Campbell, S. W., Lugaro, M., & Karakas, A. I. 2010, *A&A*, 522, L6
- Cayrel, R., Depagne, E., Spite, M., et al. 2004, *A&A*, 416, 1117
- Chiaki, G., Susa, H., & Hirano, S. 2018, *MNRAS*, 475, 4378
- Chiaki, G., Tominaga, N., & Nozawa, T. 2017, *MNRAS*, 472, L115
- Chiaki, G., Wise, J. H., Marassi, S., et al. 2020, *MNRAS*, 497, 3149
- Chiaki, G., Yoshida, N., & Hirano, S. 2016, *MNRAS*, 463, 2781
- Chon, S., Omukai, K., & Schneider, R. 2021, *MNRAS*, 508, 4175
- Claeys, J. S. W., Pols, O. R., Izzard, R. G., Vink, J., & Verbunt, F. W. M. 2014, *A&A*, 563, A83
- Clark, P. C., Glover, S. C. O., Klessen, R. S., & Bromm, V. 2011a, *ApJ*, 727, 110
- Clark, P. C., Glover, S. C. O., Smith, R. J., et al. 2011b, *Science*, 331, 1040
- Cooke, R. J., & Madau, P. 2014, *ApJ*, 791, 116
- Costa, G., Bressan, A., Mapelli, M., et al. 2021, *MNRAS*, 501, 4514
- de Mink, S. E., & Belczynski, K. 2015, *ApJ*, 814, 58
- de Souza, R. S., Yoshida, N., & Ioka, K. 2011, *A&A*, 533, A32
- Di Carlo, U. N., Mapelli, M., Giacobbo, N., et al. 2020, *MNRAS*, 498, 495
- Doi, K., & Susa, H. 2011, *ApJ*, 741, 93
- Dopcke, G., Glover, S. C. O., Clark, P. C., & Klessen, R. S. 2013, *ApJ*, 766, 103
- Downing, J. M. B., Benacquista, M. J., Giersz, M., & Spurzem, R. 2010, *MNRAS*, 407, 1946
- Edwards, D. A., & Pringle, J. E. 1987, *MNRAS*, 229, 383
- El Eid, M. F., & Langer, N. 1986, *A&A*, 167, 274
- Eldridge, J. J., Stanway, E. R., & Tang, P. N. 2019, *MNRAS*, 482, 870
- Eldridge, J. J., Stanway, E. R., Xiao, L., et al. 2017, *PASA*, 34, e058
- Farmer, R., Renzo, M., de Mink, S. E., Fishbach, M., & Justham, S. 2020, *ApJL*, 902, L36
- Farrell, E., Groh, J. H., Hirschi, R., et al. 2021, *MNRAS*, 502, L40
- Federrath, C., Sur, S., Schleicher, D. R. G., Banerjee, R., & Klessen, R. S. 2011, *ApJ*, 731, 62
- Fishbach, M., & Holz, D. E. 2020, *ApJL*, 904, L26
- Fishbach, M., Holz, D. E., & Farr, B. 2017, *ApJL*, 840, L24
- Fragione, G., & Banerjee, S. 2021, *ApJL*, 913, L29
- Fragione, G., & Kocsis, B. 2019, *MNRAS*, 486, 4781
- Fragione, G., Loeb, A., & Rasio, F. A. 2020, *ApJL*, 895, L15
- Fraleigh, G. S. 1968, *Ap&SS*, 2, 96
- Franciolini, G., Baibhav, V., De Luca, V., et al. 2021, *arXiv e-prints*, arXiv:2105.03349
- Frebel, A., & Norris, J. E. 2015, *ARA&A*, 53, 631
- Fryer, C. L., Belczynski, K., Wiktorowicz, G., et al. 2012, *ApJ*, 749, 91
- Fryer, C. L., Woosley, S. E., & Heger, A. 2001, *ApJ*, 550, 372
- Fujii, M. S., Tanikawa, A., & Makino, J. 2017, *PASJ*, 69, 94
- García, F., Simaz Bunzel, A., Chaty, S., Porter, E., & Chassande-Mottin, E. 2021, *A&A*, 649, A114
- Gerosa, D., & Berti, E. 2017, *Phys. Rev. D*, 95, 124046
- Gerosa, D., & Fishbach, M. 2021, *Nature Astronomy*, 5, 749
- Greif, T. H., Bromm, V., Clark, P. C., et al. 2012, *MNRAS*, 424, 399
- Greif, T. H., Johnson, J. L., Bromm, V., & Klessen, R. S. 2007, *ApJ*, 670, 1
- Greif, T. H., Springel, V., White, S. D. M., et al. 2011, *ApJ*, 737, 75
- Hamers, A. S., Bar-Or, B., Petrovich, C., & Antonini, F. 2018, *ApJ*, 865, 2
- Hamers, A. S., & Safarzadeh, M. 2020, *ApJ*, 898, 99
- Hartwig, T., Volonteri, M., Bromm, V., et al. 2016, *MNRAS*, 460, L74
- Heger, A., & Woosley, S. E. 2002, *ApJ*, 567, 532
- Higashi, S., Susa, H., & Chiaki, G. 2021, *ApJ*, 915, 107
- Hijikawa, K., Tanikawa, A., Kinugawa, T., Yoshida, T., & Umeda, H. 2021, *MNRAS*, 505, L69
- Hirano, S., Hosokawa, T., Yoshida, N., Omukai, K., & Yorke, H. W. 2015, *MNRAS*, 448, 568
- Hirano, S., Hosokawa, T., Yoshida, N., et al. 2014, *ApJ*, 781, 60
- Hoang, B.-M., Naoz, S., Kocsis, B., Rasio, F. A., & Dospoulou, F. 2018, *ApJ*, 856, 140
- Hong, J., Askar, A., Giersz, M., Hypki, A., & Yoon, S.-J. 2020, *MNRAS*, 498, 4287
- Hosokawa, T., Omukai, K., Yoshida, N., & Yorke, H. W. 2011, *Science*, 334, 1250
- Hurley, J. R., Tout, C. A., & Pols, O. R. 2002, *MNRAS*, 329, 897
- Hütsi, G., Raidal, M., Vaskonen, V., & Veermäe, H. 2021, *JCAP*, 2021, 068
- Inayoshi, K., Hirai, R., Kinugawa, T., & Hotokezaka, K. 2017, *MNRAS*, 468, 5020
- Inayoshi, K., Kashiyama, K., Visbal, E., & Haiman, Z. 2016, *MNRAS*, 461, 2722
- . 2021, *ApJ*, 919, 41
- Ishiyama, T., Sudo, K., Yokoi, S., et al. 2016, *ApJ*, 826, 9
- Ito, H., Aoki, W., Beers, T. C., et al. 2013, *ApJ*, 773, 33
- Johnson, J. L. 2015, *MNRAS*, 453, 2771
- Kasen, D., Woosley, S. E., & Heger, A. 2011, *ApJ*, 734, 102
- Kimball, C., Talbot, C., Berry, C. P. L., et al. 2021, *ApJL*, 915, L35
- Kinugawa, T., Inayoshi, K., Hotokezaka, K., Nakauchi, D., & Nakamura, T. 2014, *MNRAS*, 442, 2963
- Kinugawa, T., Nakamura, T., & Nakano, H. 2021a, *MNRAS*, 501, L49
- . 2021b, *Progress of Theoretical and Experimental Physics*, 2021, 021E01
- . 2021c, *MNRAS*, 504, L28
- Kremer, K., Spera, M., Becker, D., et al. 2020, *ApJ*, 903, 45
- Kresse, D., Ertl, T., & Janka, H.-T. 2021, *ApJ*, 909, 169
- Kulkarni, S. R., Hut, P., & McMillan, S. 1993, *Nature*, 364, 421
- Kumamoto, J., Fujii, M. S., & Tanikawa, A. 2020, *MNRAS*, 495, 4268
- Leigh, N. W. C., Geller, A. M., McKernan, B., et al. 2018, *MNRAS*, 474, 5672
- Leung, S.-C., Nomoto, K., & Blinnikov, S. 2019, *ApJ*, 887, 72
- Liu, B., & Bromm, V. 2020a, *MNRAS*, 495, 2475
- . 2020b, *ApJL*, 903, L40
- . 2021, *MNRAS*, 506, 5451
- Liu, B., & Lai, D. 2019, *MNRAS*, 483, 4060
- Liu, B., Meynet, G., & Bromm, V. 2021a, *MNRAS*, 501, 643
- Liu, B., Sibony, Y., Meynet, G., & Bromm, V. 2021b, *MNRAS*, 506, 5247
- Machida, M. N., & Doi, K. 2013, *MNRAS*, 435, 3283
- Machida, M. N., Omukai, K., Matsumoto, T., & Inutsuka, S.-i. 2008, *ApJ*, 677, 813
- Magg, M., Hartwig, T., Glover, S. C. O., Klessen, R. S., & Whalen, D. J. 2016, *MNRAS*, 462, 3591
- Magg, M., Klessen, R. S., Glover, S. C. O., & Li, H. 2019, *MNRAS*, 487, 486
- Mapelli, M., Giacobbo, N., Ripamonti, E., & Spera, M. 2017, *MNRAS*, 472, 2422
- Mapelli, M., Giacobbo, N., Santoliquido, F., & Artale, M. C. 2019, *MNRAS*, 487, 2
- Mapelli, M., Santoliquido, F., Bouffanais, Y., et al. 2021, *Symmetry*, 13, 1678

- Marassi, S., Chiaki, G., Schneider, R., et al. 2014, *ApJ*, 794, 100
- McKernan, B., Ford, K. E. S., & O’Shaughnessy, R. 2020, *MNRAS*, 498, 4088
- McKernan, B., Ford, K. E. S., Bellovary, J., et al. 2018, *ApJ*, 866, 66
- Müller, B., Heger, A., Liptai, D., & Cameron, J. B. 2016, *MNRAS*, 460, 742
- Nakauchi, D., Suwa, Y., Sakamoto, T., Kashiyama, K., & Nakamura, T. 2012, *ApJ*, 759, 128
- Nakazato, K., Sumiyoshi, K., & Yamada, S. 2006, *ApJ*, 645, 519
- Ng, K. K. Y., Vitale, S., Farr, W. M., & Rodriguez, C. L. 2021, *ApJL*, 913, L5
- Nomoto, K., Kobayashi, C., & Tominaga, N. 2013, *ARA&A*, 51, 457
- O’Leary, R. M., Kocsis, B., & Loeb, A. 2009, *MNRAS*, 395, 2127
- Olejak, A., Fishbach, M., Belczynski, K., et al. 2020, *ApJL*, 901, L39
- Omukai, K. 2000, *ApJ*, 534, 809
- Omukai, K., & Nishi, R. 1998, *ApJ*, 508, 141
- Paczynski, B., & Sienkiewicz, R. 1972, *Acta Astron.*, 22, 73
- Park, D., Kim, C., Lee, H. M., Bae, Y.-B., & Belczynski, K. 2017, *MNRAS*, 469, 4665
- Pejcha, O., & Thompson, T. A. 2015, *ApJ*, 801, 90
- Petrovich, C., & Antonini, F. 2017, *ApJ*, 846, 146
- Portegies Zwart, S. F., & McMillan, S. L. W. 2000, *ApJL*, 528, L17
- Pudritz, R. E., & Silk, J. 1989, *ApJ*, 342, 650
- Punturo, M., Abernathy, M., Acernese, F., et al. 2010, *Classical and Quantum Gravity*, 27, 194002
- Qin, Y., Fragos, T., Meynet, G., et al. 2018, *A&A*, 616, A28
- Rasskazov, A., & Kocsis, B. 2019, *ApJ*, 881, 20
- Rastello, S., Amaro-Seoane, P., Arca-Sedda, M., et al. 2019, *MNRAS*, 483, 1233
- Reitze, D., Adhikari, R. X., Ballmer, S., et al. 2019, in *BAAS*, Vol. 51, 35
- Rodriguez, C. L., Amaro-Seoane, P., Chatterjee, S., et al. 2018, *Phys. Rev. D*, 98, 123005
- Rodriguez, C. L., & Antonini, F. 2018, *ApJ*, 863, 7
- Ryan, S. G., Norris, J. E., & Beers, T. C. 1996, *ApJ*, 471, 254
- Sadanari, K. E., Omukai, K., Sugimura, K., Matsumoto, T., & Tomida, K. 2021, *MNRAS*, 505, 4197
- Samsing, J., Askar, A., & Giersz, M. 2018, *ApJ*, 855, 124
- Sana, H., de Mink, S. E., de Koter, A., et al. 2012, *Science*, 337, 444
- Santoliquido, F., Mapelli, M., Giacobbo, N., Bouffanais, Y., & Artale, M. C. 2021, *MNRAS*, 502, 4877
- Savonije, G. J. 1978, *A&A*, 62, 317
- Schneider, R., Ferrara, A., Salvaterra, R., Omukai, K., & Bromm, V. 2003, *Nature*, 422, 869
- Sharda, P., Federrath, C., & Krumholz, M. R. 2020, *MNRAS*, 497, 336
- Sigurdsson, S., & Hernquist, L. 1993, *Nature*, 364, 423
- Silber, K., & Tremaine, S. 2017, *ApJ*, 836, 39
- Skinner, D., & Wise, J. H. 2020, *MNRAS*, 492, 4386
- Stacy, A., Bromm, V., & Loeb, A. 2011, *MNRAS*, 413, 543
- Stone, N. C., Metzger, B. D., & Haiman, Z. 2017, *MNRAS*, 464, 946
- Suda, T., Aikawa, M., Machida, M. N., Fujimoto, M. Y., & Iben, Icko, J. 2004, *ApJ*, 611, 476
- Suda, T., Yamada, S., Katsuta, Y., et al. 2011, *MNRAS*, 412, 843
- Suda, T., Katsuta, Y., Yamada, S., et al. 2008, *PASJ*, 60, 1159
- Suda, T., Hidaka, J., Aoki, W., et al. 2017, *PASJ*, 69, 76
- Sugimura, K., Matsumoto, T., Hosokawa, T., Hirano, S., & Omukai, K. 2020, *ApJL*, 892, L14
- Sukhbold, T., Ertl, T., Woosley, S. E., Brown, J. M., & Janka, H. T. 2016, *ApJ*, 821, 38
- Sukhbold, T., Woosley, S. E., & Heger, A. 2018, *ApJ*, 860, 93
- Susa, H. 2013, *ApJ*, 773, 185
- Susa, H., Hasegawa, K., & Tominaga, N. 2014, *ApJ*, 792, 32
- Suwa, Y., & Ioka, K. 2011, *ApJ*, 726, 107
- Suwa, Y., Takiwaki, T., Kotake, K., & Sato, K. 2007a, *ApJL*, 665, L43
- . 2007b, *PASJ*, 59, 771
- . 2009, *ApJ*, 690, 913
- Tagawa, H., Haiman, Z., Bartos, I., & Kocsis, B. 2020, *ApJ*, 899, 26
- Tanikawa, A. 2013, *MNRAS*, 435, 1358
- Tanikawa, A., Kinugawa, T., Yoshida, T., Hijikawa, K., & Umeda, H. 2021a, *MNRAS*, 505, 2170
- Tanikawa, A., Susa, H., Yoshida, T., Trani, A. A., & Kinugawa, T. 2021b, *ApJ*, 910, 30
- Tanikawa, A., Yoshida, T., Kinugawa, T., Takahashi, K., & Umeda, H. 2020, *MNRAS*, 495, 4170
- Tanikawa, A., Yoshida, T., Kinugawa, T., et al. 2021c, *arXiv e-prints*, arXiv:2110.10846
- Tarumi, Y., Hartwig, T., & Magg, M. 2020, *ApJ*, 897, 58
- The LIGO Scientific Collaboration, The Virgo Collaboration, & The KAGRA Scientific Collaboration. 2021a, *arXiv e-prints*, arXiv:2111.03634
- The LIGO Scientific Collaboration, the Virgo Collaboration, the KAGRA Collaboration, et al. 2021b, *arXiv e-prints*, arXiv:2111.03606
- Tominaga, N., Iwamoto, N., & Nomoto, K. 2014, *ApJ*, 785, 98
- Trani, A. A., Rastello, S., Di Carlo, U. N., et al. 2021a, *arXiv e-prints*, arXiv:2111.06388
- Trani, A. A., Tanikawa, A., Fujii, M. S., Leigh, N. W. C., & Kumamoto, J. 2021b, *MNRAS*, 504, 910
- Turk, M. J., Abel, T., & O’Shea, B. 2009, *Science*, 325, 601
- Turk, M. J., Oishi, J. S., Abel, T., & Bryan, G. L. 2012, *ApJ*, 745, 154
- Uchida, H., Shibata, M., Takahashi, K., & Yoshida, T. 2019a, *ApJ*, 870, 98
- . 2019b, *Phys. Rev. D*, 99, 041302
- Ugliano, M., Janka, H.-T., Marek, A., & Arcones, A. 2012, *ApJ*, 757, 69
- Umeda, H., & Nomoto, K. 2002, *ApJ*, 565, 385
- . 2003, *Nature*, 422, 871
- Umeda, H., Yoshida, T., Nagele, C., & Takahashi, K. 2020, *ApJL*, 905, L21
- VanLandingham, J. H., Miller, M. C., Hamilton, D. P., & Richardson, D. C. 2016, *ApJ*, 828, 77
- Visbal, E., Bryan, G. L., & Haiman, Z. 2020, *ApJ*, 897, 95
- Wang, L., Fujii, M. S., & Tanikawa, A. 2021, *MNRAS*, 504, 5778
- Webbink, R. F. 1984, *ApJ*, 277, 355
- Woosley, S. E. 2017, *ApJ*, 836, 244
- Woosley, S. E., Blinnikov, S., & Heger, A. 2007, *Nature*, 450, 390
- Woosley, S. E., & Heger, A. 2012, *ApJ*, 752, 32
- Yamada, S., Suda, T., Komiyama, Y., Aoki, W., & Fujimoto, M. Y. 2013, *MNRAS*, 436, 1362
- Yang, Y., Bartos, I., Haiman, Z., et al. 2019, *ApJ*, 876, 122
- Yong, D., Norris, J. E., Bessell, M. S., et al. 2013, *ApJ*, 762, 26
- Yoon, J., Beers, T. C., Placco, V. M., et al. 2016, *ApJ*, 833, 20
- Yoon, S. C., Dierks, A., & Langer, N. 2012, *A&A*, 542, A113
- Yoon, S. C., Woosley, S. E., & Langer, N. 2010, *ApJ*, 725, 940
- Yoshida, N., Omukai, K., & Hernquist, L. 2008, *Science*, 321, 669
- Yoshida, T., Umeda, H., Maeda, K., & Ishii, T. 2016, *MNRAS*, 457, 351
- Zahn, J. P. 1975, *A&A*, 41, 329
- Zevin, M., Bavera, S. S., Berry, C. P. L., et al. 2021, *ApJ*, 910, 152
- Ziosi, B. M., Mapelli, M., Branchesi, M., & Tormen, G. 2014, *MNRAS*,

441, 3703